Electron Photodetachment Spectroscopy of Solvated Anions: RO·HF$^-$ or ROH·F$^-$?

Jennifer E. Mihalick,[†] Geo G. Gatev, and John I. Brauman*

Contribution from the Department of Chemistry, Stanford University, Stanford, California 94305-5080

Received December 14, 1995[⊗]

Abstract: Electron photodetachment spectra of three alkoxide ions, 2,2-dimethyl-3-pentoxide, 3,3-dimethyl-2-butoxide, trifluoroethoxide, and two complex ions, 3,3-dimethyl-2-butanol/fluoride, 2,2-dimethyl-3-pentanol/fluoride, have been measured using an ion cyclotron spectrometer to generate, trap, and detect the ions. The electron affinities of trifluoroethoxide, 2,2-dimethyl-3-pentoxide, and 3,3-dimethyl-2-butoxide were measured as 58.9 ± 0.1, 47.8 ± 0.3, and 45.7 ± 0.1 kcal mol^{-1}, respectively. Using known proton affinities of the three alcohols allows us to determine the O−H bond dissociation energies. The threshold detachment energies for 2,2-dimethyl-3-pentanol/fluoride and 3,3-dimethyl-2-butanol/fluoride complex ions are 70.3 ± 0.5, and 70.1 ± 0.5 kcal mol^{-1}, respectively. The fluoride binding energies are thus on the order of 30 kcal mol^{-1}. We show that the observation or non-observation of photodetachment for alcohol/fluoride ions depends only on the alcohol acidity. In complex ions of the form ROHF$^-$, if ROH is more acidic than HF the structure is RO$^-$·HF, and if ROH is less acidic than HF the structure is ROH·F$^-$. A flat potential energy surface model is consistent with the experimental results. The experimental results show no evidence for unusual structural change or stabilization when a hydrogen bond forms between two acids with similar acidities.

Introduction

The purpose of this work is to study the structure and energetics of gas-phase hydrogen-bonded complex anions, using alcohol/fluoride complexes as a model. The hydrogen-bonded complex between an anion and a neutral molecule is an important feature on the proton-transfer potential surface, as well as being a representative first step in solvation of the anion. We discuss the relationship between acidity and structure which affects the cross section for photodetachment via the Franck−Condon factors in these complex ions, as well as the binding energies in the neutral complexes that are produced on removal of the electron. These experiments provide an important insight into the hydrogen-bonding interactions for systems involving acids with very similar pK_a's.

The great strength of hydrogen bonds to localized anions, such as halides and alkoxides, has been demonstrated in many gas-phase thermochemical studies where the hydrogen bond energy has been shown to increase with the gas-phase acidity of the molecule and the basicity of the anion.[1−9] Measurements of the electron affinities of alcohol/fluoride complexes, in conjunction with other thermochemical data, may allow estimation of the binding energy between the ion and the neutral in the complex ion.[10,11]

In this work we use photodetachment spectroscopy to study the structure and stability of several alcohol/fluoride complexes. We have suggested previously that a relationship between acidity and geometry affects the cross section for photodetachment via the Franck−Condon factors.[10,11] The anionic proton transfer surface is relatively flat, and a small change in the acidity of the end points can produce a large geometry change. The term "flat surface" is used in this paper to describe a surface that is not parabolic, although it is, in general, not horizontal.

The geometric overlap for the adiabatic electron photodetachment transition can be quite different for fluoride complexes with alcohols more acidic than HF as compared with fluoride complexes with alcohols less acidic than HF. If there is sufficiently poor geometric overlap, the Franck−Condon factors can reduce the transition intensity so that it is below our detection sensitivity.

The structure and stability of complex ion systems have been a subject of major interest; photodetachment spectroscopy has been used to study complex ions for many years. In an early study, Golub and Steiner[12] investigated hydrogen-bonded intermediates, detached the complex ion HOHOH$^-$, and determined the relative cross section as a function of photon energy. Bowen[13] investigated the H$^-$·NH$_3$ complex ion. We[10,11] have investigated several alcohol/fluoride complexes. Neumark[14−17] has made extensive, elegant studies on bihalide complexes of the type X′HX$^-$, as well as methanol/fluoride- and ethanol/fluoride-bonded complex ions.

[†] Present address: Department of Chemistry, University of Wisconsin−Oshkosh, Oshkosh, WI.

[⊗] Abstract published in *Advance ACS Abstracts,* November 1, 1996.

(1) Arshadi, M.; Yamdagni, R.; Kebarle, P. *J. Phys. Chem.* **1970**, *74*, 1475.
(2) Kebarle, P. *Annu. Rev. Phys. Chem.* **1977**, *28*, 445.
(3) Paul, G. J.; Kebarle, P. *J. Phys. Chem.* **1990**, *94*, 5184.
(4) Bartmess, J. E. *J. Am. Chem. Soc.* **1980**, *102*, 2483.
(5) Caldwell, G.; Rozeboom, M. D.; Kiplinger, J. P.; Bartmess, J. E. *J. Am. Chem. Soc.* **1984**, *106*, 4660.
(6) Larson, J. W.; McMahon, T. B. *J. Am. Chem. Soc.* **1983**, *105*, 2944.
(7) Larson, J. W.; McMahon, T. B. *J. Am. Chem. Soc.* **1987**, *109*, 6230.
(8) Meot-Ner, M.; Sieck, L. W. *J. Phys. Chem.* **1986**, *90*, 6687.
(9) Meot-Ner, M. *J. Am. Chem. Soc.* **1986**, *108*, 6189.
(10) Moylan, C. R.; Dodd, J. A.; Brauman, J. I. *Chem. Phys. Lett.* **1985**, *118*, 38.
(11) Moylan, C. R.; Dodd, J. A.; Han, C. C.; Brauman, J. I. *J. Chem. Phys.* **1987**, *86*, 5350.
(12) Golub, S.; Steiner, B. *J. Chem. Phys.* **1968**, *49*, 5191.
(13) Coe, J. V.; Snodgrass, J. T.; Freidhoff, C. B.; McHugh, K. M.; Bowen, K. H. *J. Chem. Phys.* **1985**, *83*, 3169.
(14) Metz, R. B.; Kitsopoulos, T.; Weaver, A.; Neumark, D. M. *J. Chem. Phys.* **1988**, *88*, 1463.
(15) Weaver, A.; Metz, R. B.; Bradforth, S. E.; Neumark, D. M. *J. Phys. Chem.* **1988**, *92*, 5558.
(16) Waller, I. M.; Kitsopoulos, T. N.; Neumark, D. M. *J. Phys. Chem.* **1990**, *94*, 2240.
(17) Bradforth, S. E.; Arnold, D. W.; Metz, R. B.; Weaver, A.; Neumark, D. M. *J. Phys. Chem.* **1991**, *95*, 8066.

S0002-7863(95)04202-8 CCC: $12.00

McMahon[6] has carried out equilibrium studies on complex ions and determined the fluoride binding energies for many alcohols. Nibbering[18] carried out ion−molecule reactions of NH_4^- and deduced that its structure is a hydride ion solvated by ammonia.

These experimental studies stimulated *ab initio* calculations that were performed to describe the geometry of complex ions, as well as the energetics of the proton transfer surfaces. Computations on asymmetric proton transfer systems reveal that the shape of the surface and structure of intermediates and transition states are influenced by the relative acidities of the reaction partners. The identity of the atom involved in the hydrogen bond, e.g., a carbon, nitrogen, oxygen, or a halide, is important as well.[6,19−23]

Low-level computations on the water/fluoride and methanol/fluoride complex geometry[24,25] and high-level calculations of the potential surface of the latter system[17,26] have been performed. Based on these calculations, we expect that the results will be similar for other alcohol/fluoride complexes.[6,27] The complexes are thought to have a non-parabolic potential surface, and are asymmetric structures with the proton closer to the less acidic component. There is no evidence for a second minimum with the proton closer to the other component, separated from the first complex by a low barrier.

Our previous photodetachment study[11] on a series of alcohol/fluoride complexes showed that the acidity of the alcohol greatly affects the cross section for photodetachment of the complex ion. For five aliphatic alcohols that were less acidic than HF, the complex could not be photodetached at wavelengths greater than 360 nm. The only complex made from an alcohol more acidic than HF, benzyl alcohol, did undergo photodetachment.

Our hypothesis that the relationship between acidity and geometry affects the cross section for photodetachment via Franck−Condon factors was based on only one positive result—for benzyl alcohol which has a benzene ring, albeit non-conjugated. In the present work this hypothesis is tested more thoroughly. The electron affinities (EA's) of two alcohol/fluoride complexes made with aliphatic alcohols more acidic than HF have been measured, and their electron photodetachment spectra are reported. Inferences about the structure of the complexes are made, and the electron affinities are used in thermochemical calculations of the complex binding energies.

The thermochemical cycle requires the electron affinities of the alkoxyl radicals of those alcohols. Using our measured values of the EA's, the corresponding O−H bond dissociation energies are derived as well. Electron photodetachment spectroscopy appears to be a powerful tool for determining the neutral binding energies (NBE) for the uncharged complexes. The systems we have chosen provide an insight to the stabilization when two acids with similar acidities form a hydrogen bond.

Experimental Section

Materials. Nitrogen trifluoride was obtained from Ozark-Mahoning. Benzyl alcohol, 2,2-dimethyl-3-pentanol, 3,3-dimethyl-2-butanol, trifluoroethanol, and *N*,*O*-bis(trimethylsilyl)acetamide were purchased from Aldrich. 2,3,3-Trimethyl-2-butyl trimethylsilyl ether was synthesized from *N*,*O*-bis(trimethylsilyl)acetamide and the alcohol.[28] The TMS ether was purified by gas chromatography (HP 5790A, column SE-30, 0.25 in.). Benzyl formate was obtained from Pfaltz & Bauer. Other formate esters were synthesized from the alcohols following the procedure of Stevens.[29] 2,2-Dimethyl-3-pentyl formate and 3,3-dimethyl-2-butyl formate were recovered from the reaction mixture by extraction, while trifluoroethyl formate was separated by distillation. The 3,3-dimethyl-2-butyl formate was separated from the 3,3-dimethyl-2-butyl acetate via GC. All neutrals were further purified by several freeze−pump−thaw cycles before introduction into the high-vacuum chamber. The products were characterized by negative ion mass spectrometry by determining the mass of the alkoxide (M − 1) ion.

Ion Generation. Fluoride ion was generated by dissociative electron capture of nitrogen trifluoride, NF_3:

$$NF_3 + e^- \rightarrow F^- + NF_2 \qquad (1)$$

Alcohols were deprotonated by fluoride ion. In the case of 3,3-dimethyl-2-butanol, both 3,3-dimethyl-2-butoxide anion and the enolate anion of 3,3-dimethyl-2-butanone were observed. The enolate ion may arise from deprotonation of the ketone formed from the alcohol by dehydrogenation on the filament.[30,31] The desired alkoxide was formed cleanly when the TMS ether of the alcohol was allowed to react with fluoride ion.

Hydrogen-bonded complex ions were formed via the Riveros reaction[32,33] between a formate ester and fluoride ion:

$$HCOOR + F^- \rightarrow ROHF^- + CO \qquad (2)$$

ICR Apparatus. Experiments were performed in an ion cyclotron resonance (ICR) spectrometer,[34−36] operated in CW mode, which allows continuous ion generation and detection. This ICR instrument utilizes a single ion detector. Single-frequency phase-sensitive detection was accomplished using a home-built capacitance bridge detection (CBD) circuit, coupled to a lock-in amplifier (Princeton Applied Research Corp., Model 124A). The ion signal was digitized and averaged by an IBM PC-XT. A frequency lock system was used to correct for frequency shifts (typically ±0.1 kHz in 153 kHz) induced during photochemical experiments.[34] With typical reaction conditions the signal varies by only a few percent from the median value.

Light Sources. The ions were irradiated with light from an arc lamp or a dye laser. Low-resolution spectra were obtained using a 1000-W xenon arc lamp (Canrad-Hanovia) with long pass filters, band pass filters, or a 0.25-m high-intensity grating monochromator (Kratos Analytical). The grating was calibrated with the expanded output of a helium-neon laser and with emission lines from mercury and neon lamps. A bandwidth of 26 nm was calculated from the width of the entrance and exit slits of the monochromator and the reciprocal linear dispersion of the diffraction grating. Lamp power was measured with a thermopile (Eppley Laboratory, Inc.). Because of the configuration of the experimental setup, arc lamp power measurements could not be

(18) Kleingeld, J. C.; Ingemann, S.; Jalonen, J. E.; Nibbering, N. M. M. *J. Am. Chem. Soc.* **1983**, *105*, 2474.
(19) Sannigrahi, A. B.; Peyerimhoff, S. D. *Chem. Phys. Lett.* **1984**, *112*, 267.
(20) Cao, H. Z.; Allavena, M.; Tapia, O.; Evleth, E. M. *J. Phys. Chem.* **1985**, *89*, 1581.
(21) Gao, J.; Garner, D. S.; Jorgensen, W. L. *J. Am. Chem. Soc.* **1986**, *108*, 4784.
(22) Cybulski, S. M.; Scheiner, S. *J. Am. Chem. Soc.* **1989**, *111*, 23.
(23) Lee, T. J. *J. Am. Chem. Soc.* **1989**, *111*, 7362.
(24) Yamabe, S.; Ohtsuki, H.; Minato, T. *J. Chem. Soc., Faraday Trans. 2* **1982**, *78*, 2043.
(25) Emsley, J.; Parker, R. J.; Overill, R. E. *J. Chem. Soc., Faraday Trans. 2* **1983**, *79*, 1347.
(26) Wladkowski, B. D.; East, A. L. L.; Mihalick, J. E.; Allen, W. D.; Brauman, J. I. *J. Chem. Phys.* **1994**, *100*, 2058.
(27) Yates, B. F.; Schaefer, H. F., III; Lee, T. J.; Rice, J. E. *J. Am. Chem. Soc.* **1988**, *110*, 6327.
(28) Klebe, J. F.; Finkbeiner, H.; White, D. M. *J. Am. Chem. Soc.* **1966**, *88*, 3390.
(29) Stevens, W.; van Es, A. *Recl. Chim. Pays Bas* **1964**, 863.
(30) Caldwell, G.; Bartmess, J. E. *Int. J. Mass. Spectrom. Ion Proc.* **1981**, *40*, 269.
(31) Caldwell, G.; Bartmess, J. E. *Int. J. Mass. Spectrom. Ion Proc.* **1983**, *50*, 235.
(32) Blair, L. K.; Isolani, P. C.; Riveros, J. M. *J. Am. Chem. Soc.* **1973**, *95*, 1057.
(33) Faigle, J. F.; Isolani, P. C.; Riveros, J. M. *J. Am. Chem. Soc.* **1976**, *98*, 2049.
(34) Marks, J.; Drzaic, P. S.; Foster, R. F.; Wetzel, D. M.; Brauman, J. I.; Uppal, J. S.; Staley, R. S. *Rev. Sci. Instrum.* **1987**, *58*, 1460.
(35) Wetzel, D. M.; Brauman, J. I. *Chem. Rev.* **1987**, *87*, 607.
(36) Wetzel, D. M.; Salomon, K. A.; Berger, S.; Brauman, J. I. *J. Am. Chem. Soc.* **1989**, *111*, 3835.

performed simultaneously with the photodetachment data and were obtained separately.

High-resolution experiments were performed with a Coherent argon ion laser (Innova 200-15). Single lines in the visible region were used to bracket the threshold. The argon laser was also used to pump a continuous wave dye laser (Coherent 590). The 514-nm argon line was used with Exciton Rhodamine 560 and 590 dyes, covering the region 535 to 650 nm. The argon laser was also run on all lines in the ultraviolet to pump Exciton Exalite 392E, Exalite 400E, and Stilbene 420 dyes, producing light from 382 to 492 nm. The pump laser power at each of these wavelengths was adjusted to give approximately 60 mW output from the dye laser. This power was enough to observe photodecreases in the signal above the threshold. Wavelengths were selected with a three-plate birefringent filter. The spectral bandwidth was typically 1 cm^{-1}. The dye laser was calibrated by using the optogalvanic effect. The wavelength calibration was made by assigning optogalvanic absorptions in a calcium−neon lamp (Perkin-Elmer).[37,38]

Data Acquisition and Processing. Electron photodetachment experiments were performed by monitoring the anion population (A^-) as a function of the energy (wavelength) of irradiated light. An electron is detached from A^- when photons of sufficient energy enter the cell:

$$A^- + h\nu \rightarrow A + e^- \quad (3)$$

The electron affinity of the neutral product is determined from the location of the photodetachment threshold. Fluoride ion is a precursor for all the other anions in this study; spectra were taken only to 365 nm (78.4 kcal mol^{-1}), the detachment threshold for fluoride ion.

Data collection typically involved measuring the ion intensity without light at the beginning and the end of the scan. Signal measurements were collected at 15−50 steps. To generate an electron photodetachment spectrum we measured the fractional decrease from the steady−state ion population at each wavelength. A delay after a light change allowed the ion population to relax to the new condition; this was typically set to 1 to 10 s. A long period of data collection was chosen to average out slow oscillations in the signal level. In a typical experiment the signal was measured 10000−15000 times and the rate of data collection ranged from 8000 to 1000 Hz, giving a total time at one wavelength of 1.5 to 10 s. The number of wavelengths measured in one scan was selected to keep the time between baseline readings to about 5 min.

The relative cross section $\sigma(\lambda)$ was calculated from the fractional ion signal change, $F(\lambda)$, the wavelength, λ, and the energy of the light at that wavelength, $E(\lambda)$, using the steady state model. The relative cross section, $\sigma(\lambda)$, represents the probability of electron detachment:

$$\sigma(\lambda) = F(\lambda)/\{\lambda E(\lambda)[1 - F(\lambda)]\} \quad (4)$$

Data from each individual experiment were normalized so the sum of all cross sections was 1.0. A minimum of three scans were averaged together for each wavelength region. The averaged relative cross section files from overlapping wavelength regions were spliced together. The averaged files were normalized separately, and therefore in the splicing process they had to be scaled in order for them to have the same relative cross sections in the overlapping region.

Complex Ion Photodetachment. Complex anions were photodetached with the arc lamp and filters, and with a laser. Attempts to measure a photodetachment spectrum with the arc lamp and monochromator always produced photoincreases. To bracket the onset, a few wavelengths in the threshold region spaced by approximately 2 nm were chosen. The light-on and light-off signals were measured alternately over a period of minutes rather than seconds. The limits on the threshold were determined by finding wavelengths at which photodecreases were always observed and wavelengths at which photodecreases were never observed. Fractional decreases recorded at the high energy limit were about 5%. Fractional decreases at the low energy limit were in the order of a percent, typically oscillating at 0 ± 1%.

(37) King, D. S.; Schenk, P. K.; Smyth, K. C.; Travis, J. C. *Appl. Opt.* **1977**, *16*, 2617.

(38) Baer, S.; Brinkman, E. A.; Brauman, J. I. *J. Am. Chem. Soc.* **1991**, *113*, 805.

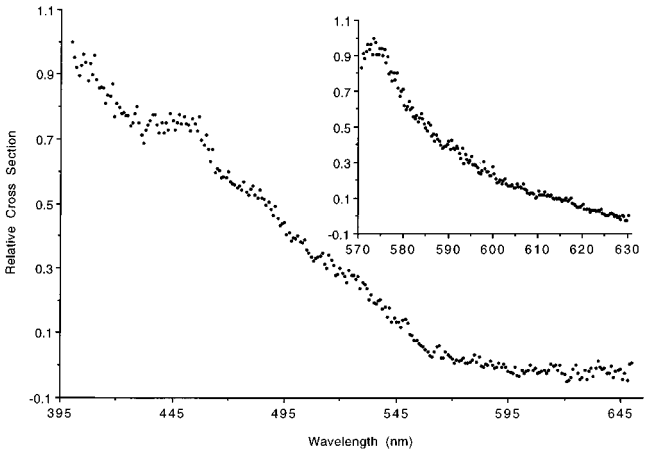

Figure 1. Arc lamp photodetachment spectrum of $(CH_3)_3CCH(CH_3)O^-$. The inset shows the laser photodetachment spectrum of $(CH_3)_3$-$CCH(CH_3)O^-$.

We observed signal increases for several ions in the threshold region when the ions were irradiated. These photoincreases, which are not fully understood, were a problem usually with the widely dispersed arc lamp radiation, which illuminated the cell plates, rather than with the laser. On some occasions we noticed that light changed the width of the cyclotron frequency distribution of the ions, so the observed change in the signal amplitude was not proportional to the actual change in population. Careful adjustment of the light position, the relative pressures of gases, and the trapping conditions reduced photoincreases, but our threshold assignments may only be upper limits to the true electron affinities.

The precision of the threshold assignment from laser photodetachment spectra was limited in part by the available laser dyes, which are rather inefficient in the threshold region. Although all three complex anions frequently showed photoincreases in the laser experiments, we were able to locate the thresholds using averaged fractional decreases from experiments that did not show photoincreases.

Results

The electron photodetachment spectra of three alkoxide anions were measured. Figure 1 shows the low-resolution arc lamp spectrum of 3,3-dimethyl-2-butoxide. The high-resolution laser spectrum is shown in the inset. The data were fit to a cubic spline function, smoothed slightly more than suggested previously.[39] The derivative reveals a progression of about 180 cm^{-1}. *tert*-Butoxide shows a progression of about 270 cm^{-1}; the lower frequency of 3,3-dimethyl-2-butoxide is plausible since we think this progression is associated with the umbrella motion of the carbinol carbon.[39] Making a crude estimate of the Franck−Condon factors from the derivative,[39] we find the best choice of the 0−0 onset is at 626 ± 1 nm (45.7 ± 0.1 kcal mol^{-1}).

Figure 2 shows the arc lamp photodetachment spectrum of 2,2-dimethyl-3-pentoxide. Photoincreases interfered with the threshold assignment, as seen from the negative cross section values. There was no problem with photoincreases in the laser experiment; the inset shows the threshold region. Straight lines were fit through different groups of data points around 600 nm, to determine the maximum and minimum possible slopes and intercepts which could represent the onset. Using this linear extrapolation of points in the threshold region the slowly rising onset is assigned as 598 ± 3 nm (47.8 ± 0.3 kcal mol^{-1}). Analysis of the derivative did not prove helpful in this analysis.

Although we observed photodetachment of trifluoroethoxide anion with the arc lamp and long pass filters, photoincreases precluded the observation of photodetachment with the mono-

(39) Janousek, B. K.; Zimmerman, A. H.; Reed, K. J.; Brauman, J. I. *J. Am. Chem. Soc.* **1978**, *100*, 6142−6148.

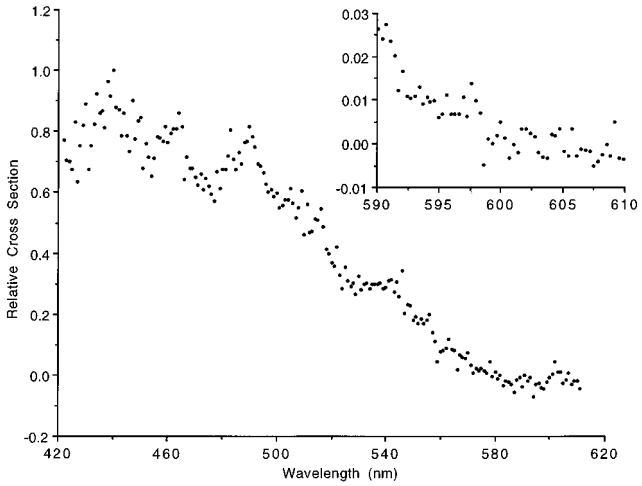

Figure 2. Arc lamp photodetachment spectrum of $(CH_3)_3CCH(C_2H_5)O^-$. The inset shows an expansion of the threshold region of the laser photodetachment spectrum of $(CH_3)_3CCH(C_2H_5)O^-$.

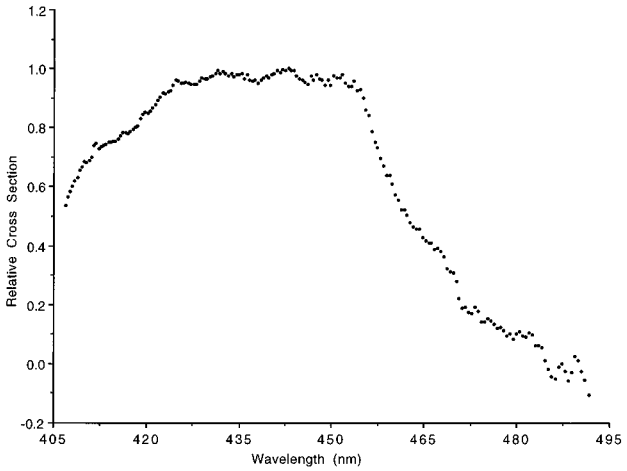

Figure 3. Laser photodetachment spectrum of $CF_3CH_2O^-$.

chromator, even using the largest slit size. Figure 3 shows the laser photodetachment spectrum. The cross section rises steeply from the threshold. The onset for photodetachment is assigned as 485.5 ± 1 nm (58.9 ± 0.1 kcal mol^{-1}). The cross section reaches a maximum about 30 nm from the onset (6 kcal mol^{-1} higher in energy) and then decreases at high photon energies. This structure has not been observed in other alkoxide spectra. Maxima have been observed in spectra of organosilanes[36] and acetophenone enolate,[40] but at much higher energies (about 2eV above the threshold). In those studies, maxima in the spectra were assigned to excited electronic states of the anion.

The threshold region for 3,3-dimethyl-2-butanol/fluoride was identified by photodetachment with the arc lamp and a 400-nm band pass filter. Figure 4 shows the laser photodetachment spectrum; the threshold is assigned at 408 ± 3 nm (70.1 ± 0.5 kcal mol^{-1}).

The threshold region for 2,2-dimethyl-3-pentanol/fluoride was identified by photodetachment with the arc lamp and a 400-nm band pass filter. The laser photodetachment data were very noisy, but showed photodetachment below 407 nm and no photodetachment above 407 nm. We assign the threshold as 407 ± 3 nm (70.3 ± 0.5 kcal mol^{-1}). Because of the noisy data, we did not attempt to derive relative cross sections. The results are consistent with those of 3,3-dimethyl-2-butanol/fluoride in which the alcohol has an acidity comparable to that of 2,2-dimethyl-3-pentanol.

(40) Jackson, R. L.; Zimmerman, A. H.; Brauman, J. I. *J. Chem. Phys.* **1979**, *71*, 2088.

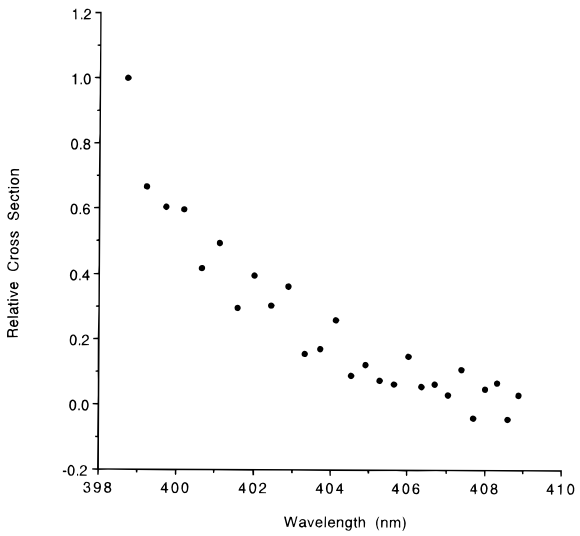

Figure 4. Laser photodetachment spectrum of $(CH_3)_3CCH(CH_3)OHF^-$.

Table 1. Experimental Results and Derived Thermochemical Data (kcal mol^{-1})

	$(CH_3)_3CCH$-$(CH_3)OH$	$(CH_3)_3CCH$-$(C_2H_5)OH$	$PhCH_2OH$	CF_3CH_2OH
EA(ROHF•)[a]	70.1 ± 0.5	70.3 ± 0.5	70.1 ± 0.5	
EA(RO•)[a]	45.7 ± 0.1	47.8 ± 0.3	49.4 ± 0.3	58.9 ± 0.1
PA(RO•)[b]	371.2 ± 2.8	370.0 ± 2.8	370.0 ± 2.8	361.9 ± 3.5
BDE (O−H)[c]	103.3 ± 2.8	104.2 ± 2.8	105.8 ± 2.8	107.2 ± 3.5
ABE[d]	34.7 ± 3.0	32.8 ± 3.1	31.0 ± 3.1	
FBE[e]	34.9 ± 4.1	33.8 ± 4.1	32.4 ± 4.1	

[a] EA ≡ electron affinity [EA(F•) = 78.4 kcal mol^{-1}]. [b] PA ≡ proton affinity [PA(F$^-$) = 371 kcal mol^{-1}]. [c] BDE ≡ bond dissociation energy of the O−H bond. [d] ABE ≡ alkoxide binding energy. [e] FBE ≡ fluoride binding energy.

In our previous study[11] the benzyl alcohol/fluoride complex was photodetached. The threshold was assigned at 408 ± 3 nm (70.1 ± 0.5 kcal mol^{-1}).

The threshold for photodetachment of the trifluoroethanol/fluoride complex anion is too high in energy for us to observe in this experiment. We expect the threshold to be at about 360 nm. The bluest laser output available to us was 385 nm (74.3 kcal mol^{-1}).

Table 1 lists measured electron affinities, the proton affinities, and the derived bond dissociation energies. Data for the benzyl alcohol complex from our previous study are included as well.

Discussion

Complex Ions and Potential Energy Surfaces. One of the goals of this work is to study the structure and the potential energy surface of complex ions. The experiment involves transitions from the anion surface to the neutral surface, which itself must be characterized. Thus we need information about the end points, the transition state(s), and the intermediates. Then based on these points and *ab initio* calculations, one can make inferences about the contours. The thermochemistry of the end points of the neutral surface is well-known and can be derived using bond dissociation energies. An alkoxyl radical and HF is lower in energy by approximately 30 kcal mol^{-1} than a fluorine atom and an alcohol. There is evidence from work of Neumark and co-workers[17,16,15] that the transition state barrier, if any, for H abstraction by fluorine atoms is low—probably no more than 3 kcal mol^{-1} above the reactants. The intermediate, the ROHF cluster, is approximately 10 kcal mol^{-1} deep (see later). The geometry of the neutral is expected to be relatively insensitive to the identity of the alcohol, because the bond

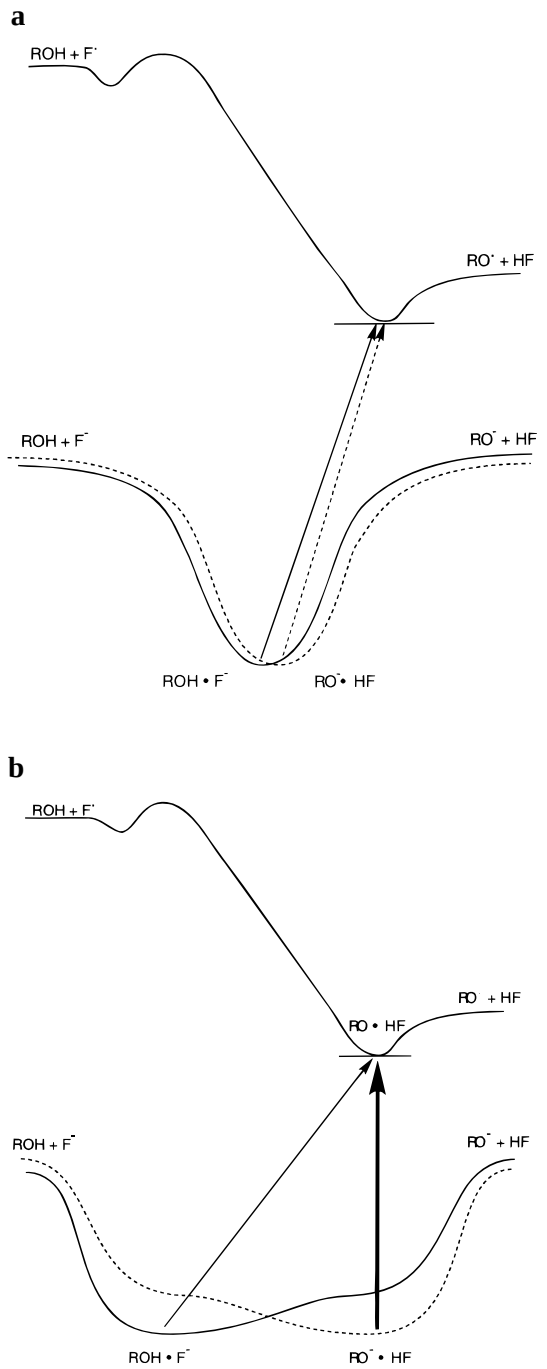

Figure 5. Schematic potential surfaces. (a) parabolic potential surface; (b) anharmonic potential surface. Although ROH·F is depicted as a minimum, there is no clear evidence for such a structure. See text.

dissociation energies of the aliphatic alcohols are similar. It is possible that there are not two distinct structures of the type RO·HF and ROH·F (see Figure 5).

The end points of the ionic potential energy surface are simply the acidities of the alcohol and HF. From studies by Moylan[41,42] we know that there is no significant barrier. He showed that the rate of proton transfer is consistent with a low barrier or no barrier at all. There are two reasonable models that might describe the surface—a parabolic potential model and a flat anionic surface model. While there is no theoretical support for the parabolic potential, theoretical evidence has been accumulated for the flat anionic surface.

(41) Moylan, C. R.; Brauman, J. I. *Annu. Rev. Phys. Chem.* **1983**, *34*, 187.

(42) Dodd, J. A.; Baer, S.; Moylan, C. R.; Brauman, J. I. *J. Am. Chem. Soc.* **1991**, *113*, 5942.

McMahon's calculations[6] on the H_2OF^- complex reveal a flat-bottomed surface. Neumark[17] has done calculations on the potential energy surface of the methanol/fluoride complex. At the Hartree−Fock (HF) level there is evidence of a plateau which disappears at the MP2 level. Finally, Wladkowski[26] has performed extensive calculations at the MP2-MP4 level on the methanol/fluoride potential surface which are in agreement with the results obtained by Neumark. They reveal that the potential surface is not parabolic but rather flat and show the "nonexistence of either a proton transfer barrier, an inflection point, or a secondary minimum of CH_3O^-·HF type".

The adiabatic energy transition between the two surfaces occurs between the ground state of the ionic surface and the ground state of the neutral surface. As the energy of the transition increases, other parts of the neutral surface become energetically accessible. The Franck−Condon factors, which include the geometrical overlap of the initial and final states give the probability of a transition as a function of the energy. Whether one sees photodetachment or not depends on the relative strengths of the transitions between the anionic and neutral surfaces. A vertical transition has the smallest geometric change, and therefore the highest intensity, of any process. If a large geometry change occurs in a transition, the Franck−Condon overlap is small, and the cross section for photodetachment decreases. In that case even if the adiabatic electron photodetachment transition is energetically accessible, a large geometry change during the process will reduce the intensity and it may not be detected.

Schematic potential energy surfaces for the parabolic and the flat anionic surface models for an alcohol/fluoride solvated anion are shown in Figures 5a and 5b, respectively. The dashed lines in Figures 5a and 5b represent the situation in which the alcohol is more acidic than HF and the solid lines show the case when the alcohol is less acidic than HF. The parabolic model predicts that a change in the energy of the end points should give a relatively small geometry change at the bottom of the well. Therefore the location of the minimum on the ionic surface of $ROHF^-$ would not depend strongly on the acidity of ROH for alcohols with similar acidity to HF. The Franck−Condon factors will be the same irrespective of whether the alcohol is more or less acidic than HF.

In contrast, the flat surface model predicts that a change in the energy of the end points will result in a large geometry change of the bottom of the well. Therefore the location of the minimum in the ionic surface of $ROHF^-$ will depend strongly on the acidity of ROH for alcohols with similar acidity to HF. When an alcohol is more acidic than HF the structure of the complex ion can be represented as RO^-·HF. When it is less acidic, the structure looks like ROH·F^-. These two geometries are significantly different and the Franck−Condon factors for them will be different. Figure 5b illustrates the behavior of a nearly flat anionic potential when the energy of the end points is changed.

The predictions from the two models can be compared with the experimental observations in our previous[11] and present studies summarized in Table 2. Complexes made from alcohols more acidic than HF, *viz.*, 2,2-dimethyl-3-butanol, benzyl alcohol, and 3,3-dimethyl-2-pentanol, have good Franck−Condon factors, and thus photodetachment can be observed at low energies. Complexes made from alcohols less acidic than HF, *viz.*, methanol, ethanol, 2-propanol, 1,1-dimethylethanol, and neopentanol do not have good Franck−Condon factors and therefore do not photodetach at low energies. The similarity in the behavior of benzyl alcohol/fluoride and the other photodetaching complexes shows that the aromatic ring in

benzyl alcohol is not the reason that this complex undergoes photodetachment. We conclude that, consistent with our hypothesis, more acidic alcohols have good Franck−Condon factors and therefore the structure of their complex ion is $RO^-\cdot HF$.

The results obtained by Neumark and co-workers[17] can be compared with the predictions of the models as well. They measured the photoelectron spectra of $MeOHF^-$ and $EtOHF^-$ ions and showed that for these alcohols which are less acidic than HF, the complex ions photodetach at high energies and the Franck−Condon factors increase with increasing energy. Neumark concluded that the structure of complexes made from alcohols less acidic than HF is $ROH\cdot F^-$.

Based on the experimental observations we conclude that for alcohols more acidic than HF the complex ions have the structure $RO^-\cdot HF$. For complex ions made from alcohols less acidic than HF the structure is $ROH\cdot F^-$. The flat surface is consistent with this model. The parabolic model can be ruled out by examining the photodetachment behavior of the neopentanol/fluoride and the 2,2-dimethyl-3-butanol/fluoride complexes. If the parabolic model were correct one would expect to observe similar photodetachment behavior for all of the complexes made of alcohols of comparable acidity. The difference in acidities between neopentanol and 2,2-dimethyl-3-butanol is only 1.5 kcal mol^{-1},[43] so their complexes would have very similar geometries and Franck−Condon factors. The neopentanol/fluoride complex does not photodetach while the 2,2-dimethyl-3-butanol/fluoride does. Thus, the parabolic potential surface does not fit the experimental observations.

Thermochemistry of Alkoxide Ions. The measured electron affinities of the alkoxide ions can be used in a thermochemical cycle to obtain other valuable information. With the alkoxyl electron affinities [EA($RO^{-\bullet}$)], the proton affinities of alkoxides [PA(RO^-)], and the ionization potential of hydrogen[43] we derive the O−H BDE for the alcohols, eq 5. The relative error in the proton affinities is estimated to be 0.2 kcal mol^{-1}.[44]

$$ROH \rightarrow RO^- + H^+ \qquad +PA(RO^-)$$

$$RO^- \rightarrow RO^\bullet + e^- \qquad +EA(RO^\bullet)$$

$$H^+ + e^- \rightarrow H^\bullet \qquad -313.57 \text{ kcal mol}^{-1}$$

$$ROH \rightarrow RO^\bullet + H^\bullet \qquad BDE$$

$$BDE = [PA(RO^-)] + [EA(RO^\bullet)] - 313.57 \qquad (5)$$

Aliphatic alcohol O−H bond dissociation energies determined experimentally cluster around 104 kcal mol^{-1}.[45,46] Our derived bond dissociation energies of 103 to 105 kcal mol^{-1} (Table 1) are within the usually observed spread for aliphatic alcohols and compare well with the accepted value of 104 kcal mol^{-1}.

The higher bond dissociation energy for trifluoroethanol at 107 kcal mol^{-1} is interesting. While this is the first O−H bond dissociation energy determination for an alcohol with electron-withdrawing substituents, similar polar effects have been found for C−H and O−O bonds. Wu and Rodgers observed an increase of 8.5 kcal mol^{-1} in the C−H bond dissociation energy for trifluoroethane as compared to ethane.[47] They explain the effect of chlorine and fluorine substituents using an electrostatic model based on work by Benson and Luria.[48] One may also consider the effect of fluorine substitution on the O−O bond dissociation energy of peroxide. Most peroxide bond energies cluster around a single value (38 kcal mol^{-1}) but the trifluoromethyl peroxide bond is more stable by 8 kcal mol^{-1}.[45] Thus, electron-withdrawing substituents have a stabilizing effect on the alkoxyl radical and other free radicals. The effect is decreased for the O−H bond in trifluoroethanol, since the fluorine substituents are β to the oxygen rather than α.

Table 2. Alcohol/fluoride Complexes: Structure and Photodetachment Behavior

R	threshold (nm)	electron affinity (kcal/mol)	Structure
methyl	not observed		$CH_3OH\cdot F^-$
ethyl	not observed		$C_2H_5OH\cdot F^-$
isopropyl	not observed		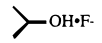
tert -butyl	not observed		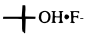
neopentyl	not observed		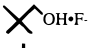
HF			
3,3-dimethyl-2-butyl	408	70.1 ± 0.5	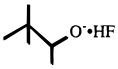
2,2-dimethyl-3-pentyl	407	70.3 ± 0.5	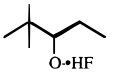
benzyl	408	70.1 ± 0.5	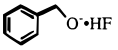

increasing ROH acidity

Thermochemistry of Complex Ions. We can obtain thermochemical information from complex ion photodetachment experiments in addition to the qualitative description of the proton transfer potential surface. Using the electron affinities of the complexes [EA($ROHF^\bullet$)] and of the alkoxyl radicals [EA($RO^\bullet$)], we obtain the difference Δ(ABE−NBE) between the binding energy of the alkoxide anion to hydrogen fluoride (ABE) and the neutral binding energy (NBE). From Δ(ABE−NBE) if we know the neutral binding energies, the alkoxide binding energy of the anion can be obtained, eq 6.

$$RO^- \rightarrow RO^\bullet + e^- \qquad +[EA(RO^\bullet)]$$

$$ROHF^\bullet + e^- \rightarrow ROHF^- \qquad -[EA(ROHF^\bullet)]$$

$$RO^\bullet + HF \rightarrow RO^\bullet HF \qquad +NBE$$

$$RO^- + HF \rightarrow ROHF^- \qquad ABE$$

$$ABE = [EA(RO^\bullet)] - [EA(ROHF^\bullet)] + NBE \qquad (6)$$

NBE is the binding energy between the neutral species, HF, and the alkoxyl radical. No experimental data are available for the binding energies for $RO^\bullet\cdot HF$ systems, but we think that the values for the related systems $ROH\cdot HF$ are a reasonable approximation. In the hydrogen bonding interaction between the alkoxyl oxygen and the HF, the oxygen shares its lone pair (not the radical center) with the proton of HF. In the $ROH\cdot HF$ system the hydrogen bonding occurs via sharing of the lone pair of the oxygen with the hydrogen from HF.[49] We assume

(43) Lias, S. G.; Bartmess, J. E.; et al. *J. Phys. Chem. Ref. Data* **1988**, *17*,

(44) Bartmess, J. E.; Scott, J. A.; McIver, R. T. *J. Am. Chem. Soc.* **1979**, *101*, 6046.

(45) McMillen, D. F.; Golden, D. M. *Annu. Rev. Phys. Chem.* **1982**, *33*, 493.

(46) Batt, L. *Int. Rev. Phys. Chem.* **1987**, *6*, 53.

(47) Wu, E. C.; Rodgers, A. S. *J. Phys. Chem.* **1974**, *78*, 2315.

(48) Benson, S. W.; Luria, M. *J. Am. Chem. Soc.* **1975**, *97*, 3342.

(49) Novoa, J. J.; Planas, M.; Whangbo, M-H.; Williams, J. M. *Chem. Phys.* **1994**, *186*, 175.

that the radical center will not significantly affect the hydrogen-bonding interaction.[50]

The binding energy in ROH·HF has not been measured experimentally, but the similar system H_2O·HF has been studied. There is, however, a range of values for the NBE in the H_2O·HF complex, as determined by different experimental and theoretical methods.

Legon[51,52] determined the equilibrium dissociation energies of H_2O·HF and reported $D_e = 10.3$ kcal mol^{-1} from absolute intensities of rotational transitions in an equilibrium mixture of water, HF, and H_2O·HF. The spread in the measurements was less than 0.2 kcal mol^{-1}. A value of 5.5 ± 1.6 kcal mol^{-1} for H_2O·HF binding energy was estimated by Thomas[53] based on IR experimental data. This value was calculated using the extinction coefficient of H_2O·HF which in turn was obtained by splitting the difference between the extinction coefficients in free HF and the much stronger ether·HF complex.

Carroll[54] performed an RHF/6-311++G**//6-31G** calculation on the H_2O·HF system and obtained a binding energy of 8.4 kcal mol^{-1}. Amos[55] performed an MP2 study on the same system and found a value of 5.5 kcal mol^{-1}. Early studies on the H_2O·HF system based on the 4-31G calculations by Morokuma[56] and Kollmann[57] produced higher values of 13.4 and 13.40 kcal mol^{-1}, respectively. The D_e values reported by Legon[51] can be compared with the values of 8.9 and 8.6 kcal mol^{-1} from *ab initio* studies performed by Szczesniak[58] and Hurst,[59] respectively.

Analyzing the shifts in the stretching vibrations Thomas predicted that the methanol−HF and the ether−HF bonds are stronger than the H_2O·HF bond. From infrared experiments Legon[60] suggests that the ROH·HF binding energy is stronger than the binding energy in H_2O·HF. Based on the analysis given above we believe that the ROH·HF binding energy is equal to or greater than 10.3 kcal mol^{-1}; we use 10.3 kcal mol^{-1} in our subsequent analysis. Owing to the range of values for the NBE of the H_2O·HF complex and the fact that the alcohol·HF complex has a stronger NBE, the associated uncertainty of this value is on the order of ± 2 kcal mol^{-1}. As we show later, 10.3 kcal mol^{-1} is probably low, and the true value is likely about 2 kcal mol^{-1} higher. Using the value of 10.3 kcal mol^{-1} of the NBE, the derived alkoxide binding energies (in kcal mol^{-1}) are listed in Table 1. Since the electron affinities of the complex anions are so similar, the differences in the calculated binding energies are solely due to the differences in alkoxyl radical electron affinities.

The alkoxide binding energy (ABE) obtained from eq 6 is the difference in energy between the complex anion and the separated alkoxide ion and hydrogen fluoride. The fluoride binding energy (FBE) is the difference in energy between the complex anion and the separated alcohol molecule and fluoride ion (Table 1). ABE and FBE are related by the energy of the proton transfer. We can compare the values of FBE with other experimental determinations of fluoride binding energies.

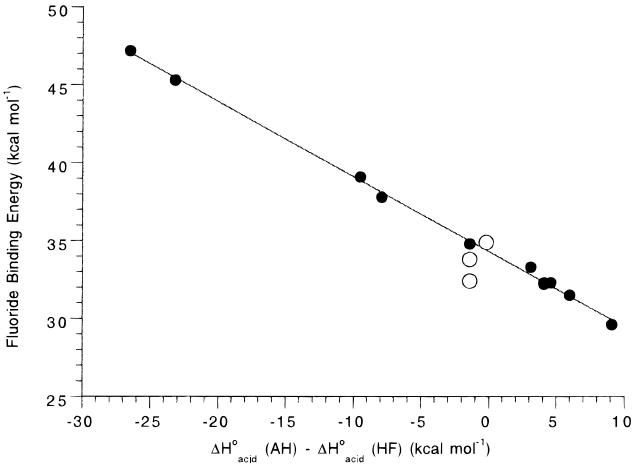

Figure 6. Fluoride binding energies vs acidities. (●) McMahon data using revised acidities from ref 42; (○) data from this work.

Although FBE of the alcohols that we investigate in the present study have not been measured previously, we can use the linear correlation between proton affinity and the fluoride binding energy for other alcohols previously discovered by Larson and McMahon.[6] Figure 6 shows the replotted McMahon data with our data added. In our previous paper[11] we reported the fluoride binding energy of the benzyl alcohol to be 31 kcal mol^{-1}. We used a value of 8 ± 2 kcal mol^{-1} for the NBE. Using our reevaluated value for NBE = 10.3 kcal mol^{-1} we arrive at a value of 33.3 kcal mol^{-1} for the ABE of benzyl alcohol/fluoride.

From the plot we can see that based on the NBE of 10.3 kcal mol^{-1}, our derived values are 0.5−2.5 kcal mol^{-1} lower than the McMahon plot. Since the NBE for the RO·HF is actually higher than the NBE for H_2O·HF, the true binding energies for our anions are in fact higher than the values plotted on the graph and are thus in better agreement with the predictions from the McMahon data for other aliphatic alcohols. The onset measurements give reliable threshold values that can be employed in thermochemical cycles. On the basis of this analysis we suspect that the "true" NBE's are approximately $11-12 \pm 2$ kcal mol^{-1}.

The nature of the hydrogen bond in the complex is of significant interest. From Figure 6 we see that the change in fluoride binding energy from one alcohol to another is approximately one-half the change in proton affinity. In the vicinity of alcohol acidities that are about the same as that of HF, the stability of ROH·F$^-$ is the same as RO$^-$·HF since there is no change in the slope of the curve. From McMahon's energetic results and our structural results, it appears that no unusual effects are present when the acidity of the alcohols is the same as that of HF. The H-bonding interaction does not show any unusual energetic or structural effect at $\Delta\Delta H_{acid} = 0$.

Implications for Hydrogen Bonds Involving Acids with Matched Acidities. Recent proposals by Gerlt[61] and Cleland and Kreevoy[62,63] on "short, strong, low barrier" hydrogen bonds

(50) The model of RO·F binding for ROH·F is imperfect, since the proton in ROH exerts a different electrostatic effect than does the electron pair in RO•. Without any quantitative information on this point, we chose the best available model. As noted below, when sufficient data exist for complex formation and photodetachment, it may be possible to evaluate these neutral binding energies more precisely.

(51) Legon, A. C.; Millen, D. J.; North, H. M. *Chem. Phys. Lett.* **1987**, *135*, 303.
(52) Legon, A. C. *Chem. Soc. Rev.* **1990**, *19*, 197.
(53) Thomas, R. K. *Proc. R. Soc., London* **1975**, *A344*, 579.
(54) Carroll, M. T.; Bader, R. F. *Mol. Phys.* **1988**, *65*, 695.
(55) Amos, R. D.; Gaw, J. F.; Handy, N. C.; Simandiras, E. D.; Somasundram, K. *Theor. Chim. Acta* **1987**, *71*, 41.
(56) Morokuma, K. *Acc. Chem. Res.* **1977**, *10*, 294.
(57) Kollmann, P.; Rothenberg, S. *J. Am. Chem. Soc.* **1977**, *99*, 1333.
(58) Szczesniak, M. M.; Scheiner, S.; Bouteiller, Y. *J. Chem. Phys.* **1984**, *81*, 5024.
(59) Hurst, G. J. B.; Fowler, P. W.; Stone, A. J.; Buckingham, A. D. *Int. J. Quantum Chem.* **1986**, *29*, 1223.
(60) Legon, A. C.; Millen, D. J.; Schrems, O. *J. Chem. Soc., Faraday Trans. 2* **1979**, *75*, 592.
(61) Gerlt, J. A.; Gassman, P. G. *Biochemistry* **1993**, *32*, 11943. Gerlt, J. A.; Gassman, P. G. *J. Am. Chem. Soc.* **1993**, *115*, 11552.
(62) Cleland, W. W.; Kreevoy, M. M. *Science* **1994**, *264*, 1887.
(63) See also: Frey, P. A.; Whitt, S. A.; Tobin, V. B. *Science* **1994**, *264*, 1927. Frey, P. A. *Science* **1995**, *264*, 189.

suggest that there is unusual stability when the hydrogen-bonding system is energetically symmetrical. These authors noted that complexation energies of ions in the gas phase can be very large, referring specifically to the stabilization of almost 30 kcal/mol for the methanol/methoxide dimer. The alcohol/fluoride complexes studied here have comparable binding energies when $\Delta\Delta H°_{acid} = 0$. Taking into account the proton transfer energy for ROH + F^- when ROH is a stronger acid than HF, the complexation energy does not appear to vary in an unusual way as the acidity of ROH and HF become equal. This is easily seen from the linearity of the Larson−McMahon plot[6] as it passes through $\Delta\Delta H° = 0$. More important, from the perspective of this paper, the structure of the complex appears to change quite dramatically when ROH becomes more acidic than HF. Thus, in the case of alcohol/fluoride complexes, the structure of the complex ion appears largely to mirror the most stable isolated structures. We observe a change from one structure to another over a very small acidity range and therefore the proton is not shared equally between the two anions. If some unusual quantum mechanical effects were occurring in the complex when the acidities were equal, we might have expected to see some interesting intermediate structure, whereas we observe nothing unusual. We infer, then, that the behavior of energetically symmetric hydrogen bonds is that expected from simple extrapolation from unsymmetric ones.

Shan, Loh, and Herschlag have shown that in solution substituted phthalic acids show no unusual energetic effects in the H-bond stabilization of their mono anions in solution as the acidities of the partners become identical.[64] Perrin[65] has shown that the structure of hydrogen-bonded complexes in solution is asymmetrical.

Conclusion

We have measured the electron affinities of three alkoxide ions, 2,2-dimethyl-3-pentoxide, 3,3-dimethyl-2-butoxide, trifluoroethoxide, and two complex ions, 3,3-dimethyl-2-butanol/fluoride and 2,2-dimethyl-3-pentanol/fluoride. We have calculated the bond dissociation energies for the alcohols and they compare well with those in similar systems. Based on the experimental results we suggest that for alcohols more acidic than HF the complex ions have the structure $RO^-{\cdot}HF$. For alcohols less acidic than HF the structure is $ROH{\cdot}F^-$. The flat potential energy surface model fits the experimental observations. The alkoxide binding energies (ABE) in these complex ions have been determined and compare well with literature data for similar systems. Electron photodetachment spectroscopy may become an important method for estimating NBE provided that reliable data from other methods are available for the ABE.

Acknowledgment. We thank the National Science Foundation for support of this research. G.G.G. gratefully acknowledges the assistance of the Salgo-Noren Foundation.

JA954202K

(64) Shan, S.; Loh, S.; Herschlag, D. *Science* **1996**, *272*, 97−101.
(65) Perrin, C. L. *Science* **1994**, *266*, 1665.